The bioelectrical source in computing single muscle fiber action potentials

Benno K. van Veen, Henk Wolters, Willemien Wallinga, Wim L. C. Rutten, and Herman B. K. Boom
University of Twente, Department of Electrical Engineering, Biomedical Engineering Division, 7500 AE Enschede, The Netherlands.

ABSTRACT Generally, single muscle fiber action potentials (SFAPs) are modeled as a convolution of the bioelectrical source (being the transmembrane current) with a weighting or transfer function, representing the electrical volume conduction. In practice, the intracellular action potential (IAP) rather than the transmembrane current is often used as the source, because the IAP is relatively easy to obtain under experimental conditions. Using a core conductor assumption, the transmembrane current equals the second derivative of the IAP. In previous articles, discrepancies were found between experimental and simulated SFAPs. Adaptations in the volume conductor slightly altered the simulation results. Another origin of discrepancy might be an erroneous description of the source. Therefore, in the present article, different sources were studied. First, an analytical description of the IAP was used. Furthermore, an experimental IAP, a special experimental SFAP, and a measured transmembrane current scaled to our experimental situation were applied. The results for the experimental IAP were comparable to those with the analytical IAP. The best agreement between experimental and simulated data was found for a measured transmembrane current as source, but differences are still apparent.

1. INTRODUCTION

The time course of a single muscle fiber action potential (SFAP) is related to the volume conduction properties of the medium, as well as to the distance between the active fiber and the recording site. Also, the bioelectrical source, in fact the active fiber impressing current to the medium, is of importance. It is generally assumed that the SFAP can be modeled as a convolution of source and transfer functions (e.g., 1–9). Most studies use a macroscopic, purely resistive, homogeneous approximation to describe volume conduction, and tissue is electrically characterized by its bulk parameters. On a microscopic scale, this approximation is not allowed: conductivity in skeletal muscle depends on the spectral characteristics of the injected current (10–13). Close to the active fiber, the frequency-dependent behavior of the muscle fiber membranes has to be taken into account. Microscopic, frequency-dependent volume conduction parameters in skeletal muscle tissue can be introduced in an electrical network model (7, 8). Such a network model has been used to calculate SFAPs (7–9, 14), and its results (9, 14) have been related to experimental results (15, 16).

In general, the resemblance between measured and computed SFAPs was still insufficient. Measured peak-to-peak voltages of SFAPs were higher (up to a factor 7) for equal recording distances and their durations were shorter (up to a factor 2). Furthermore, the shape of computed SFAPs was more dependent on the recording distance than was observed in experiments.

Several attempts have been made to explain the discrepancies between experimental and simulation results by volume conduction effects. Attention was paid to (*a*) sensitivity to changes in the network parameters (8), (*b*) capacitive properties of the T-tubular system (7), (*c*) frequency-dependent properties of the outer medium surrounding the core network part of the model (9), (*d*) muscle boundary (14), and (*e*) the presence of inhomogeneities (not yet published). However, no apparently improving effect was found either on the duration or on the shape of the computed SFAPs. In the present article, the effects of changes in the bioelectrical source will be studied.

The transmembrane current is usually considered as the bioelectrical source of SFAPs. In an approximating description, the current can be represented by a current tripole along the fiber axis (17, 18). Alternatively, the shape of the intracellular action potential (IAP) can be approximated by a synthetic Gaussian curve (19) or a quasicontinuous function (6–9, 14). The transmembrane current is then calculated as the second derivative of the IAP.

The actual transmembrane current during action potentials can be measured under in vitro conditions using the loose-patch clamp technique (20, 21). Under in vivo conditions, however, this has not proved feasible as yet. Therefore, the IAP rather than the transmembrane current is often considered as the bioelectrical source, and again the transmembrane current is equalled to the second spatial derivative of the IAP, as formulated in the linear core conductor model (e.g., 5, 22).

To investigate the effects of various current sources, we will use four different representations of the bioelectrical source. The first is a quasicontinuous representation of the transmembrane current. It is calculated as the second derivative of an analytical IAP expression (6). The second is derived from an IAP, measured under in vivo conditions (23). In source three, the membrane current is similar to an experimental SFAP. The one

Address correspondence to Dr. W. Wallinga, Department of Electrical Engineering (Biomedical Engineering Division), University of Twente, P. O. Box 217, 7500 AE Enschede, The Netherlands.

B. K. van Veen's present address is Department of Clinical Neurophysiology, Institute of Neurology, University of Nijmegen, Nijmegen, The Netherlands.

0006-3495/93/05/1492/07 $2.00

TABLE 1 **Parameter set**

Symbol	Value	Unit	Description
σ_i	0.450	$(\Omega m)^{-1}$	The intracellular conductivity
σ_e	2.500	$(\Omega m)^{-1}$	The extracellular conductivity
C_m	0.01	Fm^{-2}	The capacitance of the membrane per surface unit
G_m	1.00	$\Omega^{-1} m^{-2}$	The conductivity of the membrane per surface unit
A	$25 \cdot 10^{-6}$	m	The fiber radius
d	$1.35 \cdot 10^{-6}$	m	The thickness of the extracellular space around each fiber
p	0.9	—	The intracellular volume fraction
U	5.0	ms^{-1}	The conduction velocity
R	$1.5 \cdot 10^{-3}$	m	The radius of the muscle
α	$225 \cdot 10^{9}$	V/s^{-3}	α, β, and γ are parameters describing the intracellular action potential
β	$15 \cdot 10^{3}$	s^{-1}	
γ	0.075	V	

with the highest peak-to-peak voltage ever observed in our experiments is used as an input function. The fourth source is a direct representation of a transmembrane current as actually measured under in vitro conditions and scaled to the in vivo situation of our SFAP experiments. In all cases we used the volume conductor model presented before (14).

2. METHODS

2.1 Measured SFAPs

To validate simulation results obtained for four different bioelectrical sources, SFAPs were measured. The experimental procedure was basically the same as presented before (15). For clarity, the most important aspects will be summarized below.

Experiments were carried out in vivo on the extensor digitorum longus (EDL) muscle of the rat. The muscle was prepared free, leaving the blood supply intact. The muscle temperature was 308 ± 2 K. Activity of a fiber was evoked by penetrating the fiber with a micropipette electrode (tip diameter 1–2 μm) and applying a hyperpolarizing current pulse. No superficially lying fibers were explored. Extracellular responses were recorded with an array of 14 wire electrodes (wire diameter 25 μm). The SFAPs were low pass filtered (cutoff frequency 40 kHz, 12 dB/oct). Recordings were stored digitally after sampling at a rate of 100 kHz and A-D conversion (10 bits resolution, 4,096 samples per channel).

2.2 Source 1: membrane current based on an analytical description of the IAP

The first bioelectrical source used was based on an analytical expression for the IAP (17):

$$v_i(t) = \alpha \cdot t^3 \cdot \exp(-\beta t) - \gamma, \qquad (1)$$

with $v_i(t)$ the intracellular action potential and t the time. Parameters for α, β, and γ are listed in Table 1. Transmembrane current $i_m(t)$ was calculated according to the core conductor model (5, 22):

$$i_m(t) = f \cdot \frac{\partial^2 v_i(t)}{\partial t^2}, \qquad (2)$$

with

$$f = \frac{\pi A^2 L \sigma_i}{U^2}, \qquad (3)$$

and U the conduction velocity of the IAP, A the radius of a muscle fiber, L the length of the membrane fragment, σ_i the intracellular conductivity. Values are listed in Table 1. The conductivity parameter σ_i was chosen according to experimental data reported in literature (24, 25). The value of U was in the middle of the range, given in reference 16. The analytical IAP and the corresponding transmembrane current are depicted in Fig. 1, *A* and *B*, respectively. Throughout this study the sample interval was 10 μs. It was checked before that a further refinement of the model with shorter sample times did not change the simulation results.

2.3 Source 2: membrane current based on a recorded IAP

The second source was based on a measured IAP (23). IAPs were recorded in rat EDL muscle under the same in vivo conditions as mentioned in section 2.1. IAPs were characterized by their resting membrane potential, voltage, maximum rate of depolarization and repolarization, and rise time (defined as the time between 10 and 90% in the depolarization phase). The signal chosen in our present study is depicted in Fig. 2 *A*. Its characteristics were in the middle of the range (voltage −94 mV; rise time 0.15 ms). The second derivative was computed numerically, using a second-order procedure (26). The result, multiplied by f(Eq. 3), constituted bioelectrical source 2 (Fig. 2 *B*).

2.4 Source 3: membrane current based on large SFAP

The third source (Fig. 3) was based on a measured single fiber action potential. It is generally assumed that the SFAP voltage decreases and duration increases with extending recording distance. For this reason, the SFAP with the highest peak-to-peak voltage and the shortest duration obtained from our experiments was taken to derive source 3.

For computational reasons, the measured signal had to be transformed into a current according to:

$$i_m(t) = \kappa \cdot v_e(t), \qquad (4)$$

with $i_m(t)$ the source current, $v_e(t)$ the experimental SFAP, and κ a conversion constant, depending on the conductivity σ of the medium and the distance ρ between the active fiber and the recording site of the SFAP. However, ρ as well as σ are unknown, and therefore κ was arbitrarily chosen such that the amplitude of the current of source 3 was about equal to that of source 1.

2.5 Source 4: based on recorded membrane current

The transmembrane current was measured under in vitro conditions at a muscle fiber of the EDL of the mouse, using a loose-patch clamp technique (20, 21). A small bundle of fibers was prepared free and kept at room temperature (295 ± 2 K) in a bath with normal Ringer solution. Activity of a single fiber at the surface of the bundle was evoked by penetrating the fiber with a micropipette (tip diameter 0.5–1.0 μm) and using a hyperpolarizing current pulse (40 ms, 200–300 nA). The transmembrane current was measured using a patch pipette (tip diameter 10 μm) positioned on the surface of the fiber. Signals were sampled at a rate of 42 kHz.

An important difference in conditions between the patch clamp and

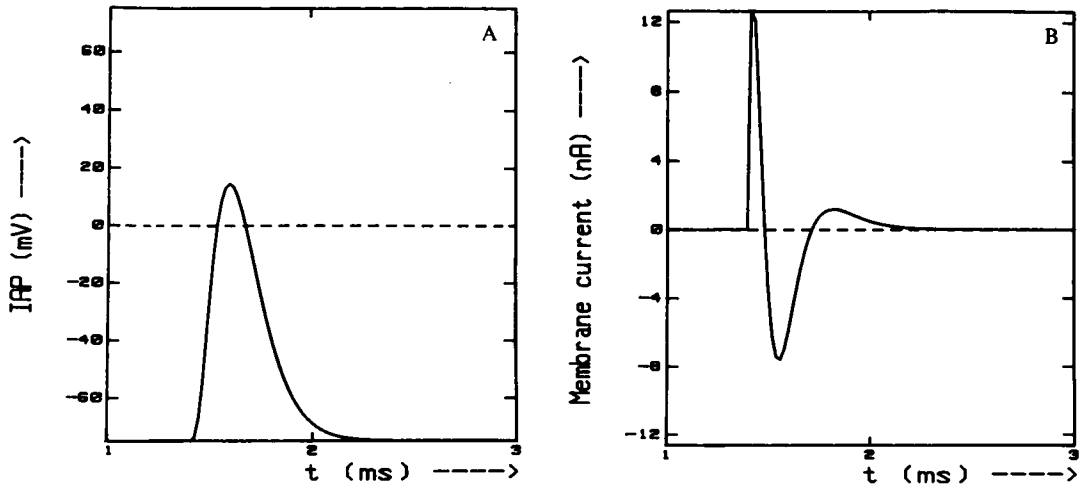

FIGURE 1 (*A*) An intracellular action potential, computed according to Rosenfalck's model. (*B*) The corresponding transmembrane current, calculated according to the core conductor theory. This signal is referred to as source 1.

the SFAP experiments is temperature. Patch clamp measurements were done at a temperature 13 K lower than the (in vivo) SFAP measurements. Because it is not exactly known how membrane currents depend on temperature, we used a detour to obtain a scaling factor. First, the patch clamp transmembrane current $i_m(t)$ was integrated twice, using Euler's method (e.g., 27). The result was multiplied by a factor $1/f$ (Eq. 3). Thus, the intracellular action potential $v_i(t)$ was computed from:

$$v_i(t) = \frac{1}{f} \cdot \int_t \left\{ \int_t i_m(t)\, dt \right\} dt. \qquad (5)$$

Then, $v_i(t)$ was compared with experimental data (23). The peak voltage of $v_i(t)$ was 110 mV, slightly larger than the voltages of the IAPs ranging between 91 and 102 mV (23). The rise time of $v_i(t)$ appeared to be much slower than the average rise time of the measured IAPs and was therefore scaled in time (scaling factor 2.6). The resulting IAP is plotted in Fig. 4 *A*. Its rise time is 0.15 ms, whereas the rise time of recorded IAPs ranged from 0.14 to 0.16 ms (23). Its maximum rates in the depolarization and repolarization phases (680 and −200 V/s, respectively) are within the experimental range. The scaled version of $i_m(t)$ (calculated according to reference 2) is plotted in Fig. 4 *B*.

2.6 Essential aspects of the calculation of SFAPs

SFAPs, $v_e(t)$, were computed as a convolution of $i_m(t)$ with a transfer function $h(t)$, where $h(t)$ is the impulse response of the volume conductor model and $i_m(t)$ one of the four sources:

$$v_e(t) = \int_{\tau=-\infty}^{t} i_m(\tau) \cdot h(t-\tau) \cdot d\tau. \qquad (6)$$

The volume conductor model accounts for the microscopic, frequency dependent, fibrous structure of muscle tissue (10). Microscopic parameters describing this structure are σ_i and σ_e (intracellular and extracellular conductivities), G_m and C_m (membrane conductance and capacitance), A (fiber radius), and d (thickness of the extracellular layer around the fibers). All fibers were assumed to have the same radius and to run parallel. The model was given a radial bound (14), with the

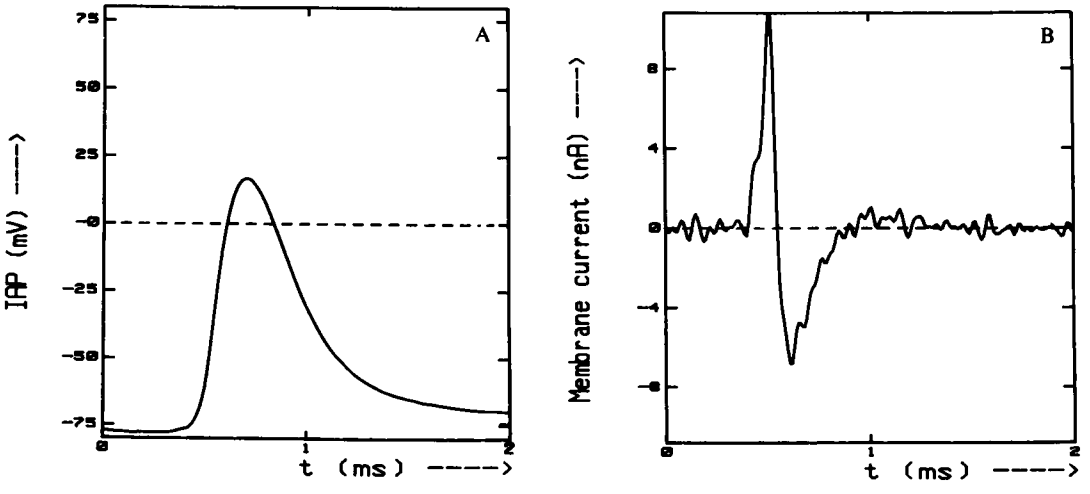

FIGURE 2 (*A*) A measured IAP, obtained from reference 23 representing a mean IAP for in vivo conditions (rat, m.EDL). (*B*) The corresponding (computed according to the core conductor theory) transmembrane current (source 2).

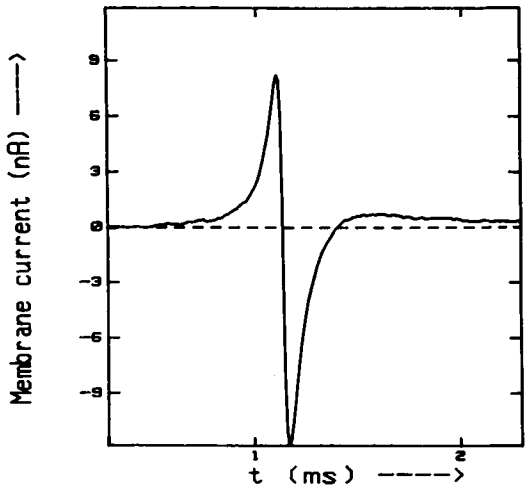

FIGURE 3 Source 3, computed from a SFAP recorded in the neighborhood of the active fiber. In this approximation no core conductor theory has been used.

radius of the total muscle model being R. Values of parameters (listed in Table 1) were chosen in the physiological range (7, 9, 14).

3. RESULTS

194 SFAPs from 40 experiments were examined. They were characterized by peak-to-peak voltage V_{tt}, the voltage of the first phase V_1, and the time interval Δt between the first and second phase (Fig. 5). Actually, these three characteristics all depend on the distance between the active fiber and the recording site, shortly recording distance. However, sufficient experimental data considering the recording distance were not available. Therefore, V_1 and Δt were both studied as function of V_{tt}. This was allowed because the three parameters are implicit functions of the recording distance. Fig. 6 presents Δt as a function of V_{tt} for every recorded SFAP. Fig. 6 shows Δt to decrease with increasing V_{tt}. Another aspect of SFAP shape was examined by relating V_1 to V_{tt} for every recorded SFAP (Fig. 7).

Simulations were done with four different descriptions of the transmembrane current, described in Methods. SFAPs were calculated for several recording distances in the range of 50–350 μm. Again, Δt and V_1 are plotted as functions of V_{tt}. In Fig.(s) 6 and 7 simulation results obtained for four different sources are compared with experimental data.

Simulation results with source 1 differed apparently from the experimental data. Simulated SFAPs had peak-to-peak voltages up to 1 mV and experimental voltages up to 5 mV (not all plotted in Figs. 6 and 7). The shortest Δt in simulated SFAPs was 140 μs and in experimental SFAPs 70 μs. Furthermore, the relation between V_1 and V_{tt} for this simulation did not agree with the relationship between V_1 and V_{tt} for experimental SFAPs.

Simulation results obtained with source 2 were, in contrast with our expectations, not improved in comparison with those of source 1. In fact, results with this source differed from the experimental data most markedly. Simulation results were also virtually the same when using another IAP (voltage 102 mV, rise time 0.16 ms) from the same set (23). Only small variations (up to 15%) in the maximum value of V_{tt} were found.

Results computed with source 3 fitted the experimental data better than those with sources 1 and 2, but V_{tt} did not reach values above 0.9 mV. Up to 0.7 mV, this source gave the best fit with respect to the V_1/V_{tt} plot. The fastest SFAP had a duration of 110 μs.

Simulation results with source 4 matched the experimental data better than the results obtained with sources

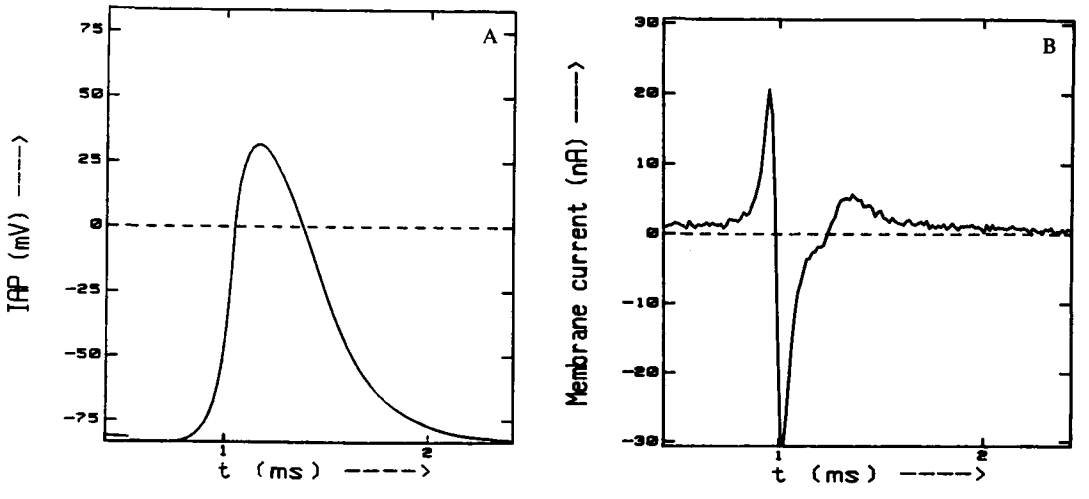

FIGURE 4 (*A*) An intracellular action potential, computed from a measured transmembrane current and scaled to the in vivo situation. (*B*) The measured transmembrane current, obtained from a loose-patch clamp experiment on a fiber in a bundle of fibers in Ringer solution (mouse, m.EDL). The signal is scaled to the in vivo situation and is referred to as source 4.

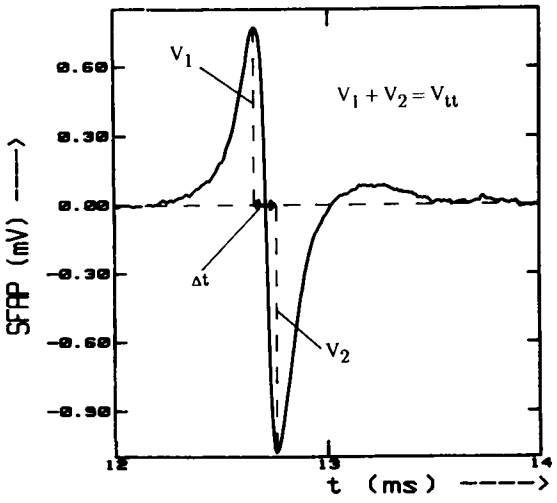

FIGURE 5 An example of an experimental SFAP. Also, Δt, V_1, and V_{tt} are indicated.

1 and 2. Peak-to-peak voltages of simulated SFAPs were up to 2 mV. The fastest Δt was 100 μs. Δt as a function of V_{tt} (Fig. 6) fitted the experimental data nicely.

The decline of V_{tt} as a function of recording distance for all source representations was studied to elaborate the source effects (Fig. 8 *A*). Here no experimental check was possible due to lack of data. The range in peak-to-peak voltages was conspicuous, whereas the decline of V_{tt} was comparable for all sources. Using source 4, voltages were more than a factor of two higher than obtained for the other sources.

In Fig. 8 *B*, the V_1/V_{tt} ratio is plotted as a function of the recording distance for simulations with all sources. For simulations with sources 1 and 2, V_1/V_{tt} decreased

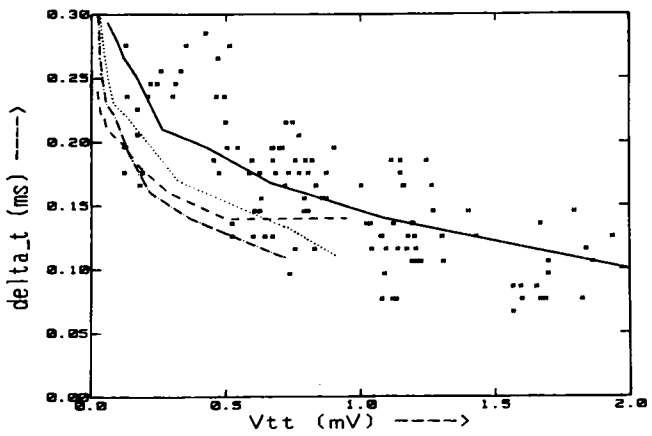

FIGURE 6 Comparison of simulations and experimental results: Δt as a function of V_{tt}. Symbols represent experimental data; (*dashed line*) result obtained with source 1; (*dashed-dotted line*) source 2; (*dotted line*) source 3; (*solid line*) source 4. The total squared difference between the experimental points and the modeled lines was for source 1 0.183; for source 2 0.253; for source 3 0.140, and for source 4 0.084 $(ms)^2$ in the V_{tt} range from 0 to 0.7 mV.

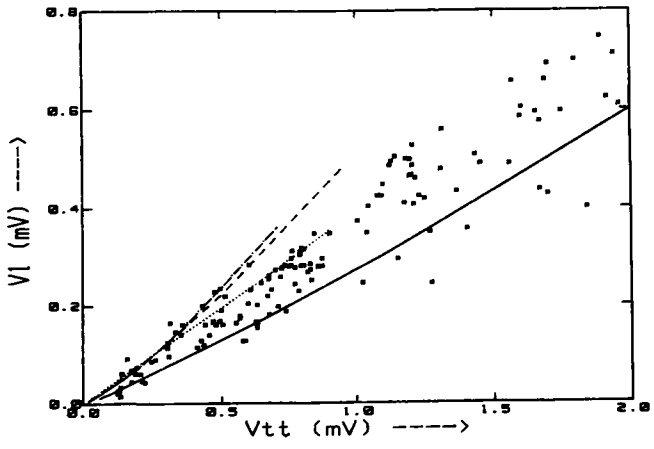

FIGURE 7 Comparison of simulations and experimental results: V_1 as a function of V_{tt}. Symbols represent experimental data; (*dashed line*) result obtained with source 1; (*dashed-dotted line*) source 2; (*dotted line*) source 3; (*solid line*) source 4. The total squared difference between the experimental points and the modeled lines was for source 1 0.230, for source 2 0.316, for source 3 0.080, and for source 4 0.125 $(mV)^2$ in the V_{tt} range from 0 to 0.7 mV.

from 0.50 close to the active fiber to 0.28 (source 2) or 0.30 (source 1) at 350 μm. With source 4, V_1/V_{tt} decreased from 0.30 to 0.24. Only for source 3, V_1/V_{tt} was independent of the recording distance, in agreement with experimental results where V_1/V_{tt} was about constant in the whole range of V_{tt} (16).

4. DISCUSSION

Several authors discussed the importance of source functions. Changes in the power spectra of simulated extracellular potentials were related to changes in conduction velocity, voltage, and duration of the IAP (3). Extracellular potentials were calculated as a convolution of a source function with a weighting function. The weighting function appeared to be strongly frequency dependent, also close to the active fiber. As a consequence, simulated extracellular potentials were not proportional to the second spatial derivative of the IAP, even in close proximity to the active fiber. The same result was experimentally found in our present study: the shape of the second derivative of the recorded IAP (Fig. 2 *B*) differs markedly from the highest recorded SFAP (Fig. 3).

Fleisher (19) used three models for the transmembrane potential: the so-called synthetic Gaussian model (where the IAP was approximated by a Gaussian function), the tripole model, and a model based on an approximation of the transmembrane potential by a sum of rectangular waves. The simulated extracellular potential results were compared with experimental data (28). With respect to the radial decline of the peak-to-peak voltage, a reasonably good agreement was found for the synthetic Gaussian model (4, 19). This agreement was achieved by varying the duration and the peak voltage of

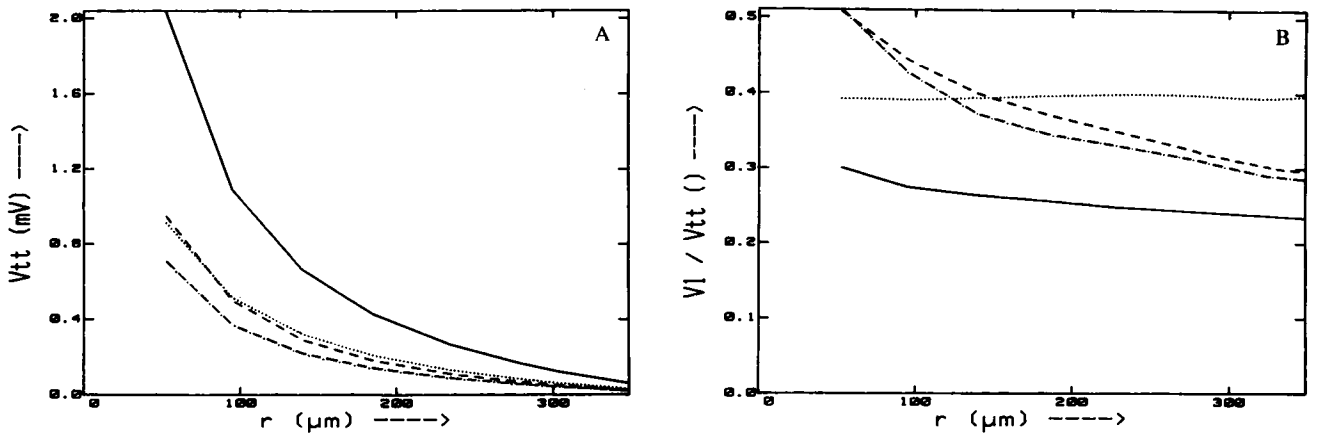

FIGURE 8 (*A*) Comparison of simulation results for the different sources: V_{tt} as a function of the recording distance. (*Dashed line*) Result obtained with source 1; (*dashed-dotted line*) source 2; (*dotted line*) source 3; (*solid line*) source 4. (*B*) Comparison of simulation results: The V_l/V_{tt} ratio as a function of the recording distance. For legends see *A*.

the function describing the IAP. The shape of the best Gaussian IAP model showed no similarity with measured IAPs (e.g., 23).

Other authors used the analytical IAP model of Rosenfalck (17) (source 1 in the present study) (6–9, 14). It was found that in general the peak-to-peak voltage of recorded SFAPs (17) was four times the voltage of simulated ones (6). Furthermore, the duration of simulated SFAPs (6) was too long: twice the duration of recorded SFAPs (17). The same discrepancy was found by van Veen et al. (9, 14) as well as in the present study (source 1). Modification of Rosenfalck's model by dividing the time scale by two enhanced the peak-to-peak voltage of the transmembrane current (proportional to the second derivative of the IAP) (6). After this transformation, the simulated data of Nandedkar and Stålberg (6) matched the experimental data. However, after this transformation, their IAP had a duration that was never obtained from experiments (23).

Rosenfalck's analytical IAP model was also used in the microscopic, frequency-dependent network model (8). Fast, as well as slow, IAP analytical expressions were derived from experimental data (23). In the case of a fast IAP in combination with a low value of the membrane capacitance C_m, the SFAP voltage was very sensitive for variations of the conduction velocity. Almost no sensitivity was found in case of a slow IAP with higher values of C_m. Although the intracellular action potential rather than the transmembrane current was used as the bioelectrical source, the importance of a reliable description of the source input function in SFAP model studies was demonstrated (8).

Differences between a measured i_m (Fig. 4 *B*) and one derived using the core conductor model (Fig.(s) 1 *B* and 2 *B*) are clear. In our patch clamp measurements, we seldomly measured an i_m with a first phase voltage larger than that of the second phase, whereas this is common for transmembrane currents computed from Rosenfalck's expression in combination with the core conductor model (source 1). The same phenomenon was found for transmembrane currents computed as the second derivative of measured IAPs (source 2).

When using a volume conductor model in conjunction with core conductor theory, the active fiber is separated from the volume conductor; the influence of the surrounding medium is neglected. Theoretically, the transmembrane current depends on the intracellular as well as the extracellular potential field, but the effect of the extracellular potential distribution will be small in case of a single active fiber in a volume conductor (29). In dog Purkinje tissue (30), it was experimentally found that the influence of the medium surrounding the active fiber could not be neglected when computing the transmembrane current. Our present study also shows that the core conductor theory is less usable for a reliable description of volume conducted SFAPs in the case of only one active fiber. Apparently, in our research, a transmembrane current measured at in vivo conditions should be used as the best possible source function.

As mentioned in the introduction, large discrepancies were found between experimental data (15, 16) and simulation results obtained from the microscopic network model in combination with Rosenfalck's IAP source (7–9, 14). In the present study, these discrepancies seem to be attenuated by introducing a more realistic source based on measured transmembrane currents. Higher simulated values of V_{tt} and shorter values for Δt were found, whereas the V_l/V_{tt} ratio was less dependent on the recording distance.

We thank Mr. Ton Verloop for manufacturing all wire electrodes.

The research was sponsored by the Foundation for Biophysics/the Netherlands Organization for Scientific Research (NWO).

Received for publication 24 March 1992 and in final form 19 January 1993.

REFERENCES

1. Plonsey, R. 1974. The active fiber in a volume conductor. *IEEE (Inst. Electr. Electron. Eng.) Trans. Biomed. Eng.* 21:371–381.
2. Dimitrov, G. V., Z. C. Lateva, and N. A. Dimitrova. 1988. Effects of changes in asymmetry, duration and propagation velocity of the intracellular potential on the power spectrum of extracellular potentials produced by an excitable fiber. *Electromyogr. Clin. Neurophysiol.* 28:93–100.
3. Dimitrov, G. V., Z. C. Lateva, and N. A. Dimitrova. 1990. Power spectra of extracellular potentials generated by an infinite, homogeneous excitable fibre. *Med. & Biol. Eng. & Comput.* 28:24–30.
4. Fleisher, S. M., M. Studer, and G. S. Moschytz. 1984. Mathematical model of the single-fibre action potential. *Med. & Biol. Eng. & Comput.* 22:433–439.
5. Clark, J., and R. Plonsey. 1968. The extracellular potential field of the single active nerve fiber in a volume conductor. *Biophys. J.* 8:842–863.
6. Nandedkar, S. D., and E. Stålberg. 1983. Simulation of single muscle fiber action potentials. *Med. & Biol. Eng. & Comput.* 21:158–165.
7. Albers, B. A., W. L. C. Rutten, W. Wallinga-de Jonge, and H. B. K. Boom. 1988a. Microscopic and macroscopic volume conduction in skeletal muscle tissue, applied to simulation of single fibre action potentials. *Med. & Biol. Eng. & Comput.* 26:605–610.
8. Albers, B. A., W. L. C. Rutten, W. Wallinga-de Jonge, and H. B. K. Boom. 1988b. Sensitivity of the amplitude of the single muscle fibre action potential to microscopic volume conduction parameters. *Med. & Biol. Eng. & Comput.* 26:611–616.
9. van Veen, B. K., W. L. C. Rutten, and W. Wallinga. 1990. The influence of a frequency-dependent medium around a network model, used for the simulation of single fiber action potentials. *Med. & Biol. Eng. & Comput.* 28:492–497.
10. Albers, B. A., W. L. C. Rutten, W. Wallinga-de Jonge, and H. B. K. Boom. 1986. A model study on the influence of structure and membrane capacitance on volume conduction in skeletal muscle tissue. *IEEE (Inst. Electr. Electron. Eng.) Trans. Biomed. Eng.* 33:681–689.
11. Gielen, F. L. H., H. E. P. Cruts, B. A. Albers, K. L. Boon, W. Wallinga-de Jonge, and H. B. K. Boom. 1986. A model of electrical conductivity of skeletal muscle tissue based on tissue structure. *Med. & Biol. Eng. & Comput.* 24:34–40.
12. Roth, B. J., F. L. H. Gielen, and J. P. Wikswo. 1988. Spatial and temporal frequency-dependent conductivities in volume-conduction calculations for skeletal muscle. *Math. Biosci.* 88:159–189.
13. Roth, B. J. 1989. Interpretation of skeletal muscle four-electrode impedance measurements using spatial and temporal frequency-dependent conductivities. *Med. & Biol. Eng. & Comput.* 27:491–495.
14. van Veen, B. K., N. J. M. Rijkhoff, W. L. C. Rutten, W. Wallinga, and H. B. K. Boom. 1992. Potential distribution and single fiber action potentials in a radially bounded muscle model. *Med. & Biol. Eng. & Comput.* 30:303–310.
15. Albers, B. A., J. H. M. Put, W. Wallinga, and P. Wirtz. 1989. Quantitative analysis of single muscle fibre action potentials recorded at known distances. *Electroencephalogr. Clin. Neurophysiol.* 73:245–253.
16. Wallinga, W., B. A. Albers, J. H. M. Put, W. L. C. Rutten, and P. Wirtz. 1988. Activity of single muscle fibres recorded at known distances. *In* Electrophysiological Kinesiology. W. Wallinga, H. B. K. Boom, and J. de Vries, editors. Elsevier Science Publishers, Amsterdam. 221–224.
17. Rosenfalck, P. 1969. Intra- and Extracellular Potential Fields of Active Nerve and Muscle Fibres. A Physicomathematical Analysis of Different Models. Akademisk Forlag, Copenhagen. 168 pp.
18. Griep, P. A. M., F. L. H. Gielen, H. B. K. Boom, K. L. Boon, L. L. W. Hoogstraten, C. W. Pool, and W. Wallinga-de Jonge. 1982. Calculation and registration of the same motor unit action potential. *Electroencephalogr. Clin. Neurophysiol.* 53:388–404.
19. Fleisher, S. M. 1984. Comparative analysis of modelled extracellular potentials. *Med. & Biol. Eng. & Comput.* 22:440–447.
20. Wolters, H., W. Wallinga, and D. L. Ypey. 1991. Recording of membrane current and action potential on the same spot in mammalian skeletal muscle fibres. *Pfluegers Arch.* 418:R152.
21. Almers, W., P. R. Stanfield, and W. Stühmer. 1983. Lateral distribution of sodium and potassium channels in frog skeletal muscle: measurements with a patch clamp technique. *J. Physiol.* 336:261–284.
22. Clark, J., and R. Plonsey. 1966. A mathematical evaluation of the core conductor model. *Biophys. J.* 6:95–112.
23. Wallinga-de Jonge, W., F. L. H. Gielen, P. Wirtz, P. de Jong, and J. Broenink. 1985. The different intracellular action potentials of fast and slow muscle fibres. *Electroencephalogr. Clin. Neurophysiol.* 60:539–547.
24. Epstein, B. R., and K. R. Foster. 1983. Anisotropy in the dielectric properties of skeletal muscle. *Med. & Biol. Eng. & Comput.* 21:51–55.
25. Zheng, E., S. Shao, and J. C. Webster. 1984. Impedance of skeletal muscle from 1 Hz to 1 MHz. *IEEE (Inst. Electr. Electron. Eng.) Trans Biomed. Eng.* 31:477–481.
26. Dahlquist, G., and O. Björck. 1974. Numerical Methods. Prentice Hall, Englewood Cliffs, NJ. 573 pp.
27. Press, W. H., B. P. Flannery, S. A. Teukolsky, and W. T. Vetterling. 1990. Numerical Recipes. The Art of Scientific Computing. Cambridge University Press, Cambridge, UK. 818 pp.
28. Andreassen, S., and A. Rosenfalck. 1981. Relationship of intracellular and extracellular action potentials of skeletal muscle fibers. *CRC Crit. Rev. Bioeng.* 6:267–306.
29. Henriquez, C. S., and R. Plonsey. 1988. The effect of the extracellular potential on propagation in excitable tissue. *Comments Theoretical Biology.* 1:47–64.
30. Spach, M. S., R. C. Barr, G. A. Serwer, J. M. Kootsey, and E. A. Johnson. 1972. Extracellular potentials related to intracellular action potentials in the dog purkinje system. *Circ. Res.* 30:505–519.